Theor Chem Account (2008) 121:83–90
DOI 10.1007/s00214-008-0452-5

REGULAR ARTICLE

Lithium–silicon Si_nLi (n = 2–10) clusters and their anions: structures, thermochemistry, and electron affinities

Ju-Cai Yang · Lihua Lin · Yousuo Zhang · Abraham F. Jalbout

Received: 28 February 2008 / Accepted: 22 April 2008 / Published online: 14 May 2008

Abstract The molecular structures, electron affinities, and dissociation energies of neutral Si_nLi (n = 2–10) species and their anions have been studied by the B3LYP and the BPW91 methods in conjunction with a DZP++ basis set. The geometries have been fully optimized with each of the proposed methods. The ground state structure of neutral Si_nLi keeps the corresponding Si_n framework unchanged. For anion, the corresponding Si_n (or Si_n^-) framework changes largely when $n \geq 7$. To evaluate the stability of the resulting anions we have calculated the adiabatic electron affinity (EA_{ad}), the vertical electron affinity (EA_{vert}), and the vertical detachment energy (VDE). The dissociating energies of Li from the lowest energy structures of neutral Si_nLi and their anions are calculated to examine relative stabilities.

Keywords Si_nLi · Electron affinities · Thermochemistry · DFT

1 Introduction

Metal-silicon clusters have attracted much attention in the past decade. This has been attributed to their intrinsic interest from the point of view of chemical structure and bonding as well as their applications in modern industry [1–5]. Specially, alkali metal silicon clusters possess scientific value because it has been known that they serve as promoters in catalysts and can be used as power source material for spaceflight aero-crafts, emitters, and many other products.

Extensive experimental and theoretical studies on alkali metal-silicon clusters have recently been reported in the literature. For example, Kaya and co-workers [6–8] have experimentally and theoretically explored the ionization potentials and electron affinities of sodium-doped silicon clusters. Zubarev et al. [9] had recently published the electron affinity of Si_6Na by means of photoelectron spectroscopy. In our group [10] we have investigated the neutral Si_nNa ($n \leq 10$) clusters and their anions by means of various density functional theory (DFT) schemes. For lithium-doped silicon clusters, Wang et al. [11] have explored the structures of Si_nLi (n = 2–7) clusters with the QCISD/6-311+G(d,p)//MP2/6-31G(d) method. Rabilloud and coworkers [12–14] reported the equilibrium geometries and electronic properties of neutral and charged $Si_nLi_p^{(+)}$ ($n \leq, p \leq 2$) species by means of MP2 and DFT methodologies. These theoretical studies primarily focus on Si_nLi clusters with small sizes ($n \leq 7$) and report their equilibrium geometries and ionization potentials.

Li et al. [15] had explored the structures of semiconductor-alkali anions E_nA^- (A = K, Na, and Li; E = Ge, Si; and n = 1–10) by means of MP2 method and predicted their vertical electron detachment energies using OVGF procedure. They suggested that the geometries of the ground state of Si_nLi^- and Si_nNa^- were identical to Si_nK^-. In fact, the geometries of Si_nA and their anions are uncertainly similar to each other. For example, the geometries of Si_9A^- [10] are not similar to each other. The geometries of Si_3A are identical. On the other hand, several isomers of Si_nK^- reported by

Electronic supplementary material The online version of this article (doi:10.1007/s00214-008-0452-5) contains supplementary material, which is available to authorized users.

J.-C. Yang (✉) · L. Lin · Y. Zhang
School of Energy and Power Engineering,
Inner Mongolia University of Technology, Hohhot 010051, China
e-mail: yangjc@imut.edu.cn

A. F. Jalbout (✉)
Department of Chemistry, The University of Arizona,
Tuson, AZ 85721, USA
e-mail: ajalbout@u.arizona.edu

Li [15] are not the lowest energy structures. All these facts spurred us to investigate Si_nLi and their anions.

When predicting molecular energies, structures, and electron affinities, there are many theoretical approaches, but considering both reliability and computational expense, gradient corrected density functional theory has been shown to be effective for predicting electron affinities of many inorganic species such as the SiH_n/SiH_n^-, $Si_2H_n/Si_2H_n^-$, GeF_n/GeF_n^-, SeF_n/SeF_n^-, and AsF_n/AsF_n^- systems [16–19]. In this report we will focus on neutral Si_nLi and their anions Si_nLi^- with n up to 10 atoms of Si in the gas phase. The methods used in this study are the carefully calibrated B3LYP and BPW91 theoretical approaches with a DZP++ basis sets. The objective of this research involves the (a) the predictions of the ground state structures of neutral Si_nLi ($n \leq 10$) and their anions; (b) the predictions of electron affinities of Si_nLi; (c) the evaluation of other properties including dissociation energies; and (d) to continue the previous work on silicon clusters [10,20,21].

2 Computational methodology

The two different density functional forms used here are (a) Becke's three-parameter hybrid exchange functional [22] with the correlation functional of Lee et al. [23] (B3LYP) and (b) Becke's 1988 exchange functional [24] with the correlation functional of Perdew and Wang [25] (BPW91).

We have selected the B3LYP method because it has been calibrated by Schaefer and coworkers [26]. They also suggested that the BPW91 method might outperform the B3LYP scheme. Alternatively, for Si_n, Si_nH, and Si_nNa clusters, the BPW91 scheme predicted the most reliable electron affinities [10,20,21]. Hence, both the B3LYP and the BPW91 schemes were implemented throughout this study. The GAUSSIAN03 suite of codes was applied for the computations [27].

A standard double-ζ plus polarization (DZP) basis set with additional diffuse functions was utilized in this work. The DZ part of the basis set was constructed from the Huzinaga [28–30], Dunning and Hay [31] set of contracted double-ζ Gaussian functions. The DZP basis set was then formed by the addition of a set of d-type polarization functions for Si and a set of p-type polarization functions for Li [α_d(Si) = 0.5000, α_p(Li) = 0.0205]. The DZP basis was augmented with diffuse functions; each atom received one additional s-type and one additional p-type functions. The diffuse function orbital exponents were determined in an "even-tempered sense" as a mathematical extension of the primitive set, according to the formula of Lee and Schaefer [32] [$\alpha_s(Si) = 0.02729, \alpha_p(Si) = 0.02500, \alpha_s(Li) = 0.00717523, \alpha_p(Li) = 0.00713759$]. The final contraction scheme for this basis set is Si (13s9p1d/7s5p1d) and Li (10s6p/5s4p). All Si_nLi and Si_nLi^- (n = 2–10) stationary point geometries were interrogated by the evaluation of their harmonic vibrational frequencies at the two different levels of theory.

The electron affinities are evaluated as the difference of total energies in the following manner: the adiabatic electron affinity is determined as EA_{ad} = E (zero-point corrected neutral) − E (zero-point corrected anion), the vertical electron affinity by EAvert = E (optimized neutral) − E (anion at optimized neutral geometry), and the vertical detachment energy of the anion by VDE = E (neutral at optimized anion geometry) − E (optimized anion).

3 Results and discussion

3.1 Si_2Li and Si_2Li^-

The geometries for the neutral Si_2Li and its anion are displayed in Fig. 1. The geometrical parameters shown in Figs. 1, 2, 3, 4, 5, 6, 7, 8, and 9 are calculated at the B3LYP level with the remainder of the parameters displayed in the supporting information. For neutral Si_2Li, Wang et al. [11], and Sporea et al. [12,14] have reported that the geometries of the ground state posses C_{2v} symmetry. Similarly Si_2H [16,33], Si_2Na [7,10], neutral Si_2Li have a $^2A_1$ ground state with a low-lying $^2B_1$ excited state. This latter state is only 0.11 and 0.16 eV higher in energy at the B3LYP and BPW91 levels of theory, respectively. The Li–Si bond lengths are predicted to be 2.615 Å at the B3LYP level of theory, which is in excellent agreement with the values of 2.63 Å predicted by the MP2/6-31G(d) method [11].

The Si_2Li^- anion displays C_{2v} symmetry with $^1A_1$ state. As we can observe from Fig. 1, the Li–Si bond lengths of anion are shorter than that of the neutral by 0.10 Å at the B3LYP level of theory. The reason (based on the reported Si_nNa system described by Kishi et al. [8]) is that the additional electron going into the SOMO of the neutral Si_nLi becomes doubly occupied in the anion, which localizes

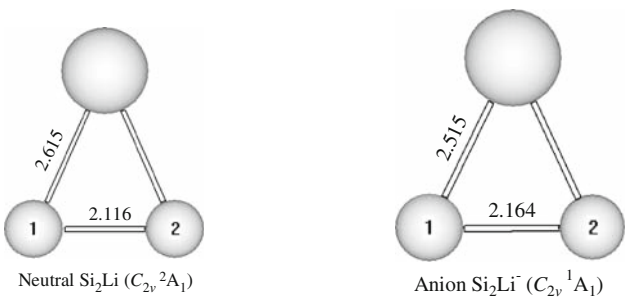

Neutral Si_2Li (C_{2v} $^2A_1$) Anion Si_2Li^- (C_{2v} $^1A_1$)

Fig. 1 The optimized geometries for neutral Si_2Li and the corresponding anion in which only silicon atoms are numbered. In the figure the B3LYP bond lengths (in Å) are shown whereas the remaining DFT parameters have been displayed in the supporting information of this article

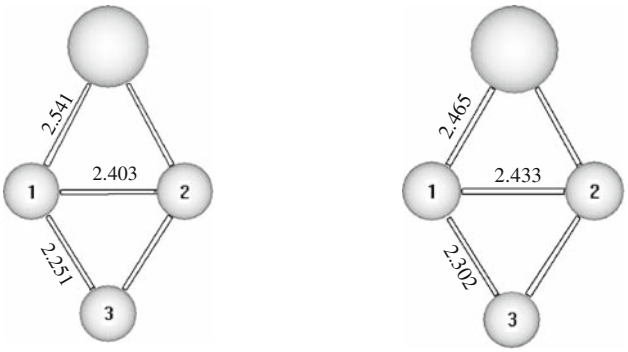

Neutral Si_3Li (C_{2v} $^2A_1$) Anion Si_3Li (C_{2v} $^1A_1$)

Fig. 2 The optimized geometries for neutral Si_3Li and the corresponding anion in which only silicon atoms are numbered. In the figure the B3LYP bond lengths (in Å) are shown whereas the remaining DFT parameters have been displayed in the supporting information of this article

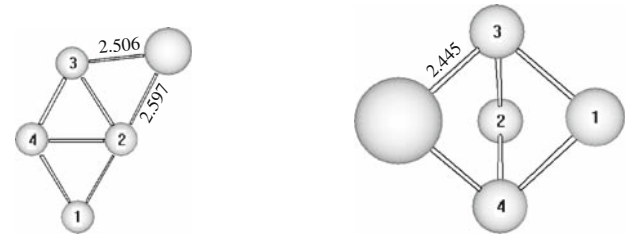

Neutral Si_4Li (C_s $^2A''$) Anion Si_4Li^- (C_{2v} $^1A_1$)

Fig. 3 The optimized geometries for neutral Si_4Li and the corresponding anion in which only silicon atoms are numbered. In the figure the B3LYP bond lengths (in Å) are shown whereas the remaining DFT parameters have been displayed in the supporting information of this article

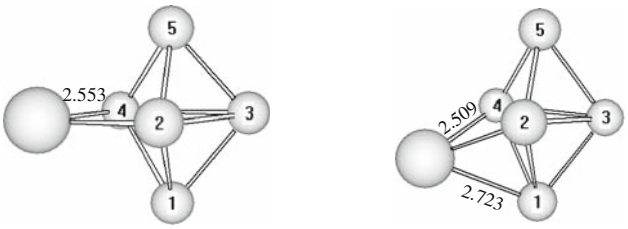

Neutral Si_5Li (C_{2v} $^2B_2$) Anion Si_5Li^- (C_s $^1A'$)

Fig. 4 The optimized geometries for neutral Si_5Li and the corresponding anion in which only silicon atoms are numbered. In the figure the B3LYP Li–Si bond lengths (in Å) are shown whereas the remaining DFT parameters have been displayed in the supporting information of this article

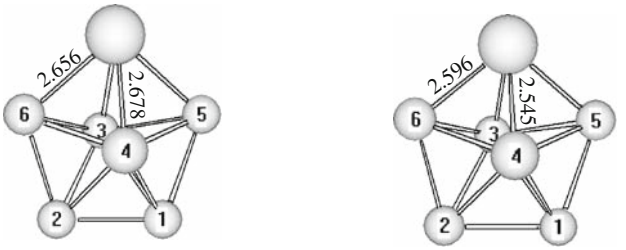

Neutral Si_6Li (C_{2v} $^2B_2$) Anion Si_6Li^- (C_{2v} $^1A_1$)

Fig. 5 The optimized geometries for neutral Si_6Li and the corresponding anion in which only silicon atoms are numbered. In the figure the B3LYP Li–Si bond lengths (in Å) are shown whereas the remaining DFT parameters have been displayed in the supporting information of this article

Neutral Si_7Li (C_{2v} $^2B_1$) Anion Si_7Li^- (C_1)

Fig. 6 The optimized geometries for neutral Si_7Li and the corresponding anion in which only silicon atoms are numbered. In the figure the B3LYP Li–Si bond lengths (in Å) are shown whereas the remaining DFT parameters have been displayed in the supporting information of this article

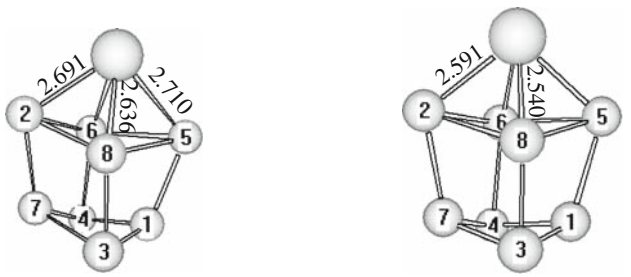

Neutral Si_8Li (C_S $^2A''$) Anion Si_8Li^- (C_{2v} $^1A_1$)

Fig. 7 The optimized geometries for neutral Si_8Li and the corresponding anion in which only silicon atoms are numbered. In the figure the B3LYP Li–Si bond lengths (in Å) are shown whereas the remaining DFT parameters have been displayed in the supporting information of this article

mainly on the Si_n framework. However, the electron back-donation from the Si_n framework to the Li atom is induced and makes the bond between the Si_n and Li atoms strong.

The theoretical neutral-anion energies for Si_nLi (n = 2–10) are listed in Table 1. The EA_{ad}, EA_{vert}, and VDE for Si_2Li are, respectively, predicted to be 1.74, 1.69, and 1.79 eV at the BPW91 level of theory, which resemble the B3LYP values. The B3LYP values are slightly larger than the BPW91 values by 0.05 eV. No experimental data are available for comparison.

3.2 Si_3Li and Si_3Li^-

The geometries of the ground state Si_3Li and its anion are displayed in Fig. 2. Previous studies have indicated that the geometries of the ground state of Si_3Li have C_{2v} symmetry [11,12,14]. Similarly Si_3H [34,35] and Si_3Na [7], the neutral

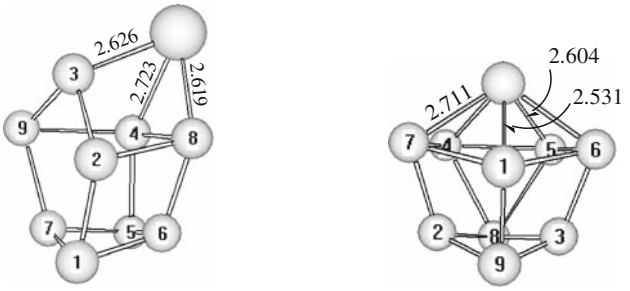

Neutral Si_9Li (C_1) Anion Si_9Li^- (C_s $^1A'$)

Fig. 8 The optimized geometries for neutral Si_8Li and the corresponding anion in which only silicon atoms are numbered. In the figure the B3LYP Li–Si bond lengths (in Å) are shown whereas the remaining DFT parameters have been displayed in the supporting information of this article

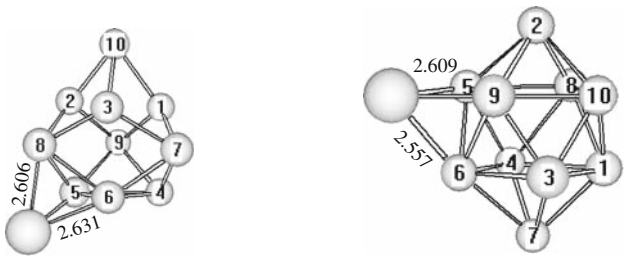

Neutral $Si_{10}Li$ (C_s $^2A'$) Anion $Si_{10}Li^-$ (C_s $^1A'$)

Fig. 9 The optimized geometries for neutral $Si_{10}Li$ and the corresponding anion in which only silicon atoms are numbered. In the figure the B3LYP Li–Si bond lengths (in Å) are shown whereas the remained of the DFT parameters have been displayed in the supporting information of this article

Si_3Li has a $^2A_1$ ground state with a low-lying $^2B_2$ excited state. Again, the latter state is only higher in energy by 0.15 and 0.14 eV at the B3LYP and BPW91 levels of theory, respectively. The Li–Si bond lengths are calculated to be 2.541 Å at the B3LYP level of theory, which are in agreement with the values of 2.55 Å predicted at the MP2/6-31G(d) level of theory [11]. For the negatively charged ion Si_3Li^-, the ground state structure has C_{2v} symmetry with $^1A_1$ state. The Li–Si bond lengths of anion Si_3Li^- are shorter than that of neutral by 0.08 Å at the B3LYP level. The reason is described earlier.

For Si_3Li, the EA_{ad}, EA_{vert}, and VDE are 1.98, 1.96, and 2.04 eV at the BPW91 level of theory, respectively. As can be seen from Table 1, the B3LYP values are in good agreement with the BPW91 values, but again lack of experimental data prevents us from making a methodological recommendation.

3.3 Si_4Li and Si_4Li^-

The geometries of the ground state structures Si_4Li and its anions are displayed in Fig. 3. The ground state structure for Si_4Li is C_s symmetry with $^2A''$ state which is in agreement with previous theoretical studies [11,12,14]. The ground-state structure of Si_4Li is different from that of Si_4Na, which has C_{2v} symmetry with $^2B_2$ state. It is also different from Si_4H [7,10]. In fact, the H–Si bonds for ground state structures of Si_nH with the exception of Si_2H and Si_3H are stretched bonds. However, the R–Si bonds for ground state geometries of Si_nR are bridged. The Li–Si bond lengths of Si_4Li are predicted to be 2.506 and 2.597 Å at the B3LYP level of theory, that is in agreement with values of 2.50 and 2.60 Å predicted by the MP2/6-31G(d) theory method [11]. For the negatively charged ion Si_4Li^-, the ground state structure has C_{2v} symmetry with $^1A_1$ state. Therefore, the most stable isomer of Si_4Li^- differs from that of neutral Si_4Li. The Li–Si bond lengths of Si_4Li^- are predicted to be 2.445 Å at the B3LYP level of theory.

The theoretical EA_{ad}, EA_{vert}, and VDE for Si_4Li are predicted to be 1.84, 1.25, and 2.39 eV at the BPW91 level of theory, and 1.78, 1.18, and 2.39 eV at the B3LYP level of theory, respectively. The B3LYP values are close to the BPW91 values. The values of EA_{ad}, EA_{vert}, and VDE are different from each other on account of the large change in geometry between the neutral cluster and its anion.

3.4 Si_5Li and Si_5Li^-

The geometries of ground state Si_5Li and its anion are displayed in Fig. 4. For the neutral Si_5Li cluster, Sporea et al.

Table 1 The zero-point corrected adiabatic electron affinity (EA_{ad}), the vertical electron affinity (EA_{vert}), and the vertical detachment energy (VDE) for the Si_nLi ($n = 2$–10) clusters, all of which are in units of eV

Species	Method	EA_{ad}	EA_{vert}	VDE
$Si_2Li(^2A_1 \leftarrow ^1 A_1)$	B3LYP	1.79	1.74	1.83
	BPW91	1.74	1.69	1.79
$Si_3Li(^2A_1 \leftarrow ^1 A_1)$	B3LYP	1.97	1.94	2.03
	BPW91	1.98	1.96	2.04
$Si_4Li(^2A'' \leftarrow ^1 A_1)$	B3LYP	1.78	1.18	2.41
	BPW91	1.84	1.25	2.39
$Si_5Li(^2A' \leftarrow ^1 A')$	B3LYP	2.46	2.05	2.85
	BPW91	2.45	2.03	2.83
$Si_6Li(^2A' \leftarrow ^1 A')$	B3LYP	2.24	2.14	2.37
	BPW91	2.24	2.15	2.36
$Si_7Li(^2B_2 \leftarrow ^1 C_1)$	B3LYP	2.23	1.46	2.71
	BPW91	2.23	1.42	2.75
$Si_8Li(^2B_2 \leftarrow ^1 A_1)$	B3LYP	2.98	2.72	3.22
	BPW91	2.98	2.76	3.19
$Si_9Li(^1C_1 \leftarrow ^1 A')$	B3LYP	2.90	2.27	3.21
	BPW91	3.01	2.27	3.20
$Si_{10}Li(^2A' \leftarrow ^1 A')$	B3LYP	2.82	2.24	3.40
	BPW91	2.73	2.19	3.33

[12,14] reported that the geometries of the ground state displayed C_s symmetry at the B3LYP/6-31+G(d) level of theory. Wang et al. [11] reported that it was C_{2v} symmetry with the MP2/6-31G(d) method. Our DFT computations reveal that this structure has the C_{2v} symmetry with $^2B_2$ state at the BPW91 level of theory. At the B3LYP level of theory, there is an imaginary frequency with a b_2 mode to be found for the C_{2v} symmetry structure. Following the $b_2$mode, the C_{2v} symmetry collapses to C_s symmetry with $^2A'$ state. The C_{2v} and the C_s geometry have essentially the same energies The C_{2v} structure is only higher in energy than the C_s structure by 0.00009 eV (0.002 kcal/mol). On the other hand, the small imaginary frequencies of 12 cm^{-1} for the C_{2v} structure are thought to be an artifact of the numerical integration. Hence, we assign the C_{2v} symmetry for the ground state geometry of Si_5Li at the B3LYP level of theory which is identical to the MP2 result. The Li–Si bond lengths of Si_5Li are predicted to be 2.553 Å at the B3LYP level of theory, which are in agreement with values of 2.52 Å predicted by MP2/6-31G(d) [11].

For the negatively charged Si_5Li^- ion, the ground state structure has C_s symmetry in the $^1A'$ state. The Li–Si bond lengths of Si_5Li^- are predicted to be 2.509 and 2.723 Å at the B3LYP level of theory, respectively. The theoretical EA_{ad}, EA_{vert}, and VDE for Si_5Li are predicted to be 2.45, 2.03, and 2.83 eV at the BPW91 level of theory, respectively. As can be seen from Table 1, the B3LYP values are in good agreement with the BPW91 values. The values of EA_{ad}, EA_{vert}, and VDE are different from each other because of the large change in geometry between neutral cluster and its anion.

3.5 Si_6Li and Si_6Li^-

The C_{2v}-symmetry structure of the $^2B_2$ ground state for neutral Si_6Li and the C_{2v}-symmetry structure of the $^1A_1$ ground state for anion Si_6Li^- are displayed in Fig. 5. For neutral Si_6Li, our DFT results agree with earlier theoretical studies [11,12,14]. The two equivalent Li–Si bond lengths are predicted to be 2.656 Å and another two equivalent Li–Si bond lengths are predicted to be 2.678 Å at the B3LYP level of theory, which are in agreement with values of 2.62 and 2.68 Å predicted by MP2/6-31G(d), respectively [11]. These Li–Si bond lengths in anion are shortened from neutral structure by 0.06 and 0.13 Å, respectively.

Our DFT results for Si_6Li^- are different from the earlier studies reported by Li et al. [15] They asserted that Si_6A^- (A = Li, Na, and K) clusters displayed C_{3v} symmetry (see [15] for the C_{3v} symmetry structure). Energetically, the C_{3v}-symmetry isomer for Si_6Li^- is less stable than the C_{2v}-symmetry by 0.47 and 0.63 eV at the B3LYP and the BPW91 levels of theory, respectively. Further computations on Si_6K^- at the MP2(full)/6-311+G(d) and B3LYP/6-311+G(d) levels of theory reveal that the C_{3v} symmetry isomers are local minima on the potential energy surface of Si_6K^-. The C_{2v} symmetry structures for Si_6K^- are more stable in energy than the C_{3v} symmetry by 0.20 and 0.07 eV at MP2(full)/6-311+G(d) and B3LYP/6-311+G(d) levels of theory, respectively. For Si_6Na^-, the ground state structure is also C_{2v} symmetry [8–10,15]. That is, the C_{3v} symmetry isomers are local minima points on the potential energy surface of Si_6A^-. As can be seen from Table 1, both the BPW91 and the B3LYP values of EA_{ad}, EA_{vert}, and VDE for Si_6Li are in excellent agreement and predicted to be 2.24, 2.15, and 2.36 eV, respectively.

3.6 Si_7Li and Si_7Li^-

The C_{2v}-symmetry structures of the $^2B_1$ ground state for neutral Si_7Li and the C_1-symmetry ground state structures for the Si_7Li^- anion are displayed in Fig. 6. For the neutral Si_7Li, our DFT results agree with earlier theoretical studies [11]. The two equivalent Li–Si bond lengths are predicted to be 2.554 Å at the B3LYP level of theory, which are in agreement with values of 2.56 Å predicted by MP2/6-31G(d) [11].

For Si_7Li^-, the ground state geometries are *distorted rhombohedron* with C_1 symmetry. This result is different from the previous study reported by Li et al. [15]. They presented that Si_7A^- (A = Li, Na, and K) clusters had C_s symmetry (see [15] for the C_s symmetry structure). Energetically, the C_s-symmetry isomer for Si_7Li^- is less stable than the C_1-symmetry by 0.35 and 0.40 eV at the B3LYP and the BPW91 levels of theory, respectively. Again, further computation on Si_7K^- with the MP2(full)/6-311+G(d) and B3LYP/6-311+G(d) schemes show that they are C_1 symmetry structures. This species is more stable in energy than the C_s symmetry by 0.22 and 0.04 eV at MP2(full)/6-311+G(d) and B3LYP/6-311+G(d) levels of theory, respectively. For Si_7Na^-, the ground state structure is also *distorted rhombohedron* with C_1 symmetry [10]. That is, the C_s symmetry isomers are local minima points on the potential energy surface of Si_7A^-.

As can be seen from Table 1, both the BPW91 and the B3LYP values of EA_{ad}, EA_{vert}, and VDE for Si_7Li are in excellent agreement. The theoretical EA_{ad}, EA_{vert}, and VDE are predicted to be 2.23, 1.42, and 2.75 eV (BPW91 values), respectively. The values of EA_{ad}, EA_{vert}, and VDE are, again, different from each other due to the large changes in geometry between the neutral cluster and its anion.

3.7 Si_8Li and Si_8Li^-

The C_s-symmetry structure of the $^2A''$ ground state for neutral Si_8Li and the C_{2v}-symmetry structure of the $^1A_1$ ground state for anion Si_8Li^- are displayed in Fig. 7. For the Si_8Li

neutral structure, the two equivalent Li–Si, Li–2Si, and Li–2Si bond lengths are predicted to be 2.636, 2.691, and 2.710 Å at the B3LYP level of theory, respectively.

For Si_8Li^-, the Li–Si bond lengths are shorter than corresponding bonds in neutral by 0.10 Å. One can note that the DFT results are different from the previous study reported by Li et al. [15]. They presented that the Si_8A^- clusters had C_1 symmetry. In fact, the C_1 structures for Si_8K^- are less stable in energy than the C_{2v} symmetry by 0.63 and 0.91 eV at MP2(full)/6-311+G(d) and B3LYP/6-311+G(d) levels of theory, respectively. That is, the ground state geometries for Si_8A^- display C_{2v} symmetry with $^1A_1$ state (for Si_8Na^-, see [10]). The C_1 symmetry isomers are local minima points on the potential energy surface of Si_8A^-.

As can be seen from Table 1, both the BPW91 and the B3LYP values of EA_{ad}, EA_{vert}, and VDE for Si_8Li are, again, in excellent agreement. The theoretical EA_{ad}, EA_{vert}, and VDE are predicted to be 2.98, 2.76, and 3.19 eV (BPW91 values), respectively.

3.8 Si_9Li and Si_9Li^-

The C_1-symmetry ground state structure for neutral Si_9Li and C_s-symmetry structure of the $^1A'$ ground state for anion Si_9Li^- are displayed in Fig. 8. For Si_9Li, the three Li–Si bond lengths are predicted to be 2.626, 2.723, and 2.619 Å at the B3LYP level of theory, respectively. For Si_9Li^-, the two equivalent Li–6Si and Li–7Si bond distances are predicted to be 2.711 Å, the two equivalent Li–4Si and Li–5Si bond distances are predicted to be 2.604 Å, and the Li–1Si bond lengths are predicted to be 2.531 Å at the B3LYP level of theory. The ground state structures of Si_9Li^- differ from those of Si_9K^- that have C_{3v} symmetry structures [15,20]. The theoretical EA_{ad} for Si_9Li are predicted to be 2.90 and 3.01 eV at the B3LYP and the BPW91 levels of theory, respectively. The EA_{vert} and VDE are predicted to be 2.27 and 3.20 eV at both the B3LYP and the BPW91 levels of theory, respectively.

3.9 $Si_{10}Li$ and $Si_{10}Li^-$

The C_s-symmetry structure of the $^2A'$ ground state for $Si_{10}Li$ and C_s-symmetry structure of the $^1A'$ ground state for $Si_{10}Li^-$ are displayed in Fig. 9. For neutral $Si_{10}Li$, the two equivalent Li–5Si and Li–6Si bond lengths are predicted to be 2.631 Å and the Li–8Si bond distances are predicted to be 2.606 eV at the B3LYP level of theory. It is useful to mention that Majumder [36] studied the impurity-doped Si_{10} cluster and Sporea and Rabilloud [37] reported stability of alkali-encapsulating silicon cage clusters. For $Si_{10}Li^-$, the two equivalent Li–5Si and Li–9Si bond lengths are predicted to be 2.609 Å, and the Li–6Si bond distances are predicted to be 2.557 eV at the B3LYP level of theory.

The theoretical EA_{ad}, EA_{vert}, and VDE for $Si_{10}Li$ are predicted to be 2.73, 2.19, and 3.33 eV at the BPW91 level of theory, respectively. The B3LYP values are slightly larger than those of the BPW91 by 0.07 eV seen in Table 1. The values of EA_{ad}, EA_{vert}, and VDE are, again, different from each other due to the large change in geometry between neutral cluster and its anion seen in Fig. 9.

It is interesting to note that the ground state structure for neutral Si_nLi keeps the Si_n framework unchanged [11,12]. For Si_nLi^-, the ground state structure also keeps the corresponding Si_n (or Si_n^-) framework unchanged when $n \leq 6$, while the corresponding Si_n (or Si_n^-) framework changes largely when $n \geq 7$. For electron affinities, the values predicted by the B3LYP and the BPW91 are very close. This result may indicate that the electron affinity predicted by these methods is right and close to experimental value because actual electron affinity is the one and only.

3.10 Dissociation energies

The dissociation energy (D_e) (defined as the energy required in the reaction $Si_nLi \rightarrow Si_n$+Li) for Si_nLi species are evaluated and exhibited in Table 2. Rabilloud and coworkers [12] calculated the D_e for Si_nLi with n from 1 to 6. As can be seen from Table 2, the energy difference between the B3LYP and the BPW91 values is within 0.10 eV. In Fig. 10, the BPW91 D_e for Si_nLi and Si_nNa (see [10]) as a function of the size of the clusters is shown. As can be seen from Fig. 10, the two parallel oscillating curves, the top curve for Si_nLi and the lower curve for Si_nNa, show that (i) the dissociation energies are local minima for $n = 4$ and 7, and local maxima for $n = 2$, 5, and 8. In other words, Si_nLi and Si_nNa for $n = 4$ and 7 are less stable than when $n = 2$, 5 and 8. These also indicate that Si_n for $n = 4$ and 7 are more stable and for $n = 2$, 5, and 8 are less stable. This result is consistent with previous results with respect to Si_n [20,38,39] (ii) as expected the dissociation energies of lithium atom are larger than that of sodium. That is, Li adsorption on surface of silicon clusters is more stable than Na. This result is in agreement with experimental observations [17]. The reason is that the small size of Li atoms results in a higher stability.

The D_e (defined as the energy required in the reaction $Si_nLi^- \rightarrow Si_n^-$+Li) of Si_nLi^- cluster is also calculated and is displayed in Table 3. The BPW91 D_e for the Si_nLi^- and Si_nNa^- (see [10]) as a function of the size of the clusters is also shown in Fig. 11. The energies difference between the B3LYP and the BPW91 values are within 0.08 eV seen in Table 3. The top curve in Fig. 11 shows that the De of Si_nLi^- is local minima for $n = 4$ and 7 and local maxima for $n = 2$, 5, and 9. That is, Si_4Li^- and Si_7Li^- are less stable and Si_2Li^-, Si_5Li^-, and Si_9Li^- are more stable. The two curves in Fig. 11 also show that the dissociation energies

Table 2 Dissociation energies (D_e) for the Neutral Si_nLi ($n = 2$–10) clusters in eV. The values displayed in *parenthesis* correspond to zero-point vibrational energies. It is also useful to note that the B3LYP and the BPW91 calculations on the ground state structures of Si_n have been presented in [20]

Dissociation	B3LYP	BPW91
$Si_2Li \rightarrow Si_2+Li$	2.33 (2.29)	2.43 (2.39)
$Si_3Li \rightarrow Si_3+Li$	2.20 (2.16)	2.19 (2.15)
$Si_4Li \rightarrow Si_4+Li$	1.63 (1.60)	1.73 (1.70)
$Si_5Li \rightarrow Si_5+Li$	2.16 (2.12)	2.25 (2.12)
$Si_6Li \rightarrow Si_6+Li$	1.89 (1.85)	2.00 (1.95)
$Si_7Li \rightarrow Si_7+Li$	1.45 (1.41)	1.39 (1.37)
$Si_8Li \rightarrow Si_8+Li$	2.17 (2.11)	2.19 (2.14)
$Si_9Li \rightarrow Si_9+Li$	1.78 (1.72)	1.70 (1.65)
$Si_{10}Li \rightarrow Si_{10}+Li$	1.67 (1.64)	1.66 (1.63)

Table 3 Dissociation energies (D_e) for the Si_nLi^- ($n = 2$–10) anions in units of eV. The values displayed in parenthesis correspond to zero-point vibrational energies. As in the previous table, the B3LYP and the BPW91 computed results for the ground state structures of Si_n have been presented in [20]

Dissociation	B3LYP	BPW91
$Si_2Li^- \rightarrow Si_2^-+Li$	2.06 (2.02)	2.01 (1.98)
$Si_3Li^- \rightarrow Si_3^-+Li$	1.85 (1.79)	1.87 (1.81)
$Si_4Li^- \rightarrow Si_4^-+Li$	1.27 (1.22)	1.33 (1.29)
$Si_5Li^- \rightarrow Si_5^-+Li$	2.15 (2.10)	2.19 (2.15)
$Si_6Li^- \rightarrow Si_6^-+Li$	2.01 (1.95)	2.14 (2.08)
$Si_7Li^- \rightarrow Si_7^-+Li$	1.58 (1.53)	1.58 (1.53)
$Si_8Li^- \rightarrow Si_8^-+Li$	2.28 (2.20)	2.35 (2.27)
$Si_9Li^- \rightarrow Si_9^-+Li$	2.37 (2.31)	2.45 (2.39)
$Si_{10}Li^- \rightarrow Si_{10}^-+Li$	2.02 (1.98)	1.94 (1.90)

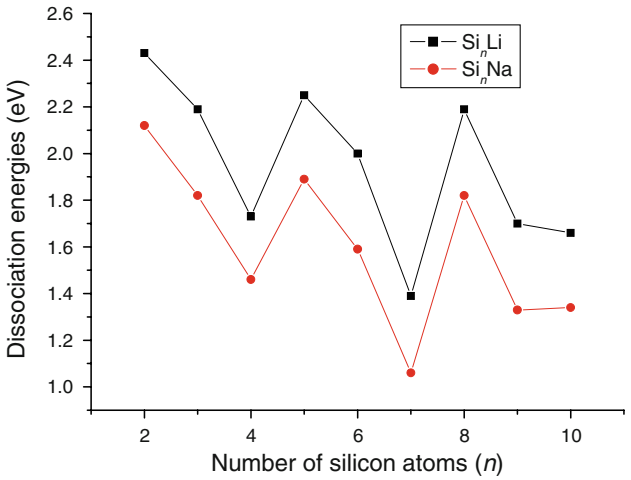

Fig. 10 Dissociation energies (computed using uncorrected zero-point vibrational energies) of Si_nR ($Si_nR \rightarrow Si_n+R$) (where R = Li, Na and as for Si_nNa, see [10]) calculated using the BPW91 method and plotted versus the number of atoms n in the clusters

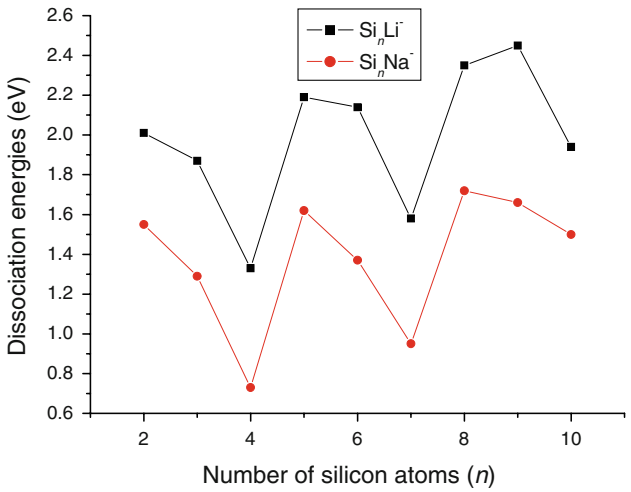

Fig. 11 Dissociation energies (uncorrected with zero-point vibrational energies) of Si_nR ($Si_nR^- \rightarrow Si_n^-+R$) (where R = Li, Na and as for Si_nNa^-, see [10]) calculated using the BPW91 method and plotted versus the number of atoms n in the clusters

of lithium atom are larger than that of sodium. The reason is described above.

4 Conclusions

The present work has provided a systematic study of the Si_nLi/Si_nLi^- clusters with two carefully selected DFT methods. The lowest energy structures of these clusters have been reported, and we have focused on the neutral Si_nLi clusters with n from 8 to 10 and anions Si_nLi^- with n up to 10. The predicted ground state structure is believable when compared with MP2 level of theory. The ground state structures of the neutral Si_nLi clusters keep the corresponding Si_n framework. For Si_nLi^-, the lowest energy structures also keep the corresponding Si_n (or Si_n^-) framework unchanged when $n \leq 6$, while the corresponding Si_n framework is modified when $n \geq 7$. The ground state structures of Si_nK^- ($n = 6$, 7, and 8) have been modified when compared with Si_nLi^-. The adiabatic electron affinity, the vertical electron affinity, and the vertical detachment energy for Si_nLi have been estimated. The values predicted by the B3LYP and the BPW91 schemes are very close. The dissociation energies of Li from the lowest energy structures of Si_nLi/Si_nLi^- ($n = 2$–10) have been calculated and used to understand relative stability. To the best of our knowledge, there are no experimental data regarding the adiabatic electron affinity and dissociation for these systems. Our results may thus provide a reference for further investigations.

Acknowledgments We would like to thank Prof. Henry F. Schaefer III and Dr. Yaoming Xie for kindly offering the DZP++ basis sets which have been employed for the lithiums and silicon atoms. This work has been financially supported by a research grant (Grant No. NJ05052) administered by the Science and Research Foundation of Higher Education of Inner Mongolia and by the NCET Grant (Grant No. NCET-06-0267) from the Ministry of Education of the People's Republic of China.

References

1. Beck SM (1989) J Chem Phys 90:6306
2. Ohara M, Koyasu K, Nakajima A, Kaya K (2003) Chem Phys Lett 371:490
3. Binning RCJr, Bacelo DE (2005) J Phys Chem A 109:754
4. Koyasu K, Akutsu M, Mitsui M, Nakajima A (2005) J Am Chem Soc 127:4998
5. Jaeger JB, Jaeger TD, Duncan MA (2006) J Phys Chem A 110:9310
6. Kaya K, Sugioka T, Taguwa T, Hoshino K, Nakajima AZ (1993) Phys D 26:S 201
7. Kishi R, Iwata S, Nakajima A, Kaya K (1997) J Chem Phys 107:3056
8. Kishi R, Kawamata H, Negishi Y, Iwata S, Nakajima A, Kaya K (1997) J Chem Phys 107:10029
9. Zubarev DY, Alexandrova AN, Boldyrev AI, Cui LF, Li X, Wang LS (2006) J Chem Phys 124:124305
10. Lin LH, Yang JC, Ning HM, Hao DS, Fan HW (2008) J Mol Struct (Theochem) 851:197
11. Wang H, Lu WC, Li ZS, Sun CC (2005) J Mol Struct (Theochem) 730:263
12. Sporea C, Rabilloud F, Cosson X, Allouche AR, Aubert-Frécon M (2006) J Phys Chem A 110:6032
13. Sporea C, Rabilloud F, Allouche AR, Frécon M (2006) J Phys Chem A 110:1046
14. Sporea C, Rabilloud F, Aubert-Frécon M (2007) J Mol Struct THEOCHEM 802:85
15. Li SD, Ren GM, Jin ZH (2003) J Chem Phys 119:10063
16. Pak C, Rienstra-Kiracofe JC, Schaefer HF (2000) J Phys Chem A 104:11232
17. Li QS, Xu WG, Xie Y, Schaefer HF (1999) J Chem Phys 111:7945
18. Li QS, Xu WG, Xie Y, Schaefer HF (1999) J Phys Chem A 103:7496
19. Xu WG, Li GL, Yu G, Zhao Y, Li QS, Xie Y, Scheafer HF (2003) J Phys Chem A 107:258
20. Yang JC, Xu WG, Xiao WS (2005) J Mol Struct THEOCHEM 719:89
21. Yang JC, Bai X, Li CP, Xu WG (2005) J Phys Chem A 109:5717
22. Becke AD (1993) J Chem Phys 98:5648
23. Lee C, Yang W, Parr RG (1988) Phys Rev B 37:785
24. Becke AD (1988) Phys Rev A 38:3098
25. Perdew JP, Wang Y (1992) Phys Rev B 45:13244
26. Rienstra-Kiracofe JC, Tschumper GS, Schaefer HF, Nandi S, Ellison G (2002) B Chem Rev 102:231
27. Gaussian 03, Revision C.02, Frisch MJ, Trucks GW, Schlegel HB, Scuseria GE, Robb MA, Cheeseman JR, Montgomery Jr. JA, Vreven T, Kudin KN, Burant JC, Millam JM, Iyengar SS, Tomasi J, Barone V, Mennucci B, Cossi M, Scalmani G, Rega N, Petersson GA, Nakatsuji H, Hada M, Ehara M, Toyota K, Fukuda R, Hasegawa J, Ishida M, Nakajima T, Honda Y, Kitao O, Nakai H, Klene M, Li X, Knox JE, Hratchian HP, Cross JB, Bakken V, Adamo C, Jaramillo J, Gomperts R, Stratmann RE, Yazyev O, Austin AJ, Cammi R, Pomelli C, Ochterski JW, Ayala PY, Morokuma K, Voth GA, Salvador P, Dannenberg JJ, Zakrzewski VG, Dapprich S, Daniels AD, Strain MC, Farkas O, Malick DK, Rabuck AD, Raghavachari K, Foresman JB, Ortiz JV, Cui Q, Baboul AG, Clifford S, Cioslowski J, Stefanov BB, Liu G, Liashenko A, Piskorz P, Komaromi I, Martin RL, Fox DJ, Keith T, Al-Laham MA, Peng CY, Nanayakkara A, Challacombe M, Gill PMW, Johnson B, Chen W, Wong MW, Gonzalez C, Pople JA (2004) Gaussian Inc., Wallingford
28. Huzinaga SJ (1965) Chem Phys 42:1293
29. Dunning TH Jr (1970) J Chem Phys 53:2823
30. Huzinaga S (1971) Approximate atomic wavefunctions, vol II. Department of Chemistry, University of Alberta, Edmonton, AB, Canada
31. Dunning TH, Hay PJ (1977) Modern theoretical chemistry. In: Schaefer HF (ed) Plenum, New York, Chap 1, pp 1–27
32. Lee TJ, Schaefer HF (1985) J Chem Phys 83:1784
33. Kalcher J, Sax AF (1993) Chem Phys Lett 215:601
34. Xu C, Taylor TR, Burton GR, Neumark DM (1998) J Chem Phys 108:7645
35. Xu WG, Yang JC, Xiao WS (2004) J Phys Chem A 108:11345
36. Majumder C, Kulshreshtha SK (2004) Phys Rev B 70:245426
37. Sporea C, Rabilloud F (2007) J Chem Phys 127:164306
38. Raghavachari K (1986) J Chem Phys 84:5672
39. Raghavachari K, Rohlfing CM (1988) J Chem Phys 89:2219